Contribution from the Division of Chemical and Physical Sciences, Deakin University, Waurn Ponds, 3217 Victoria, Australia,
and Department of Inorganic Chemistry, University of Melbourne, Parkville, 3052 Victoria, Australia

Influence of Isomeric Form, Chelated Ring Size, and the Metal on the Oxidation of Facial and Meridional Chromium, Molybdenum, and Tungsten Tricarbonyl Bis(bis(diphenylphosphino)methane) and Bis(1,2-bis(diphenylphosphino)ethane) Complexes

Alan M. Bond,*[1] Ray Colton,*[2] and Katherine McGregor[2]

Received November 15, 1985

A series of complexes of the kind $M(CO)_3(\eta^1\text{-P-P})(\eta^2\text{-P-P})$ (M = Cr, Mo, W; P-P = $Ph_2PCH_2PPh_2$ (dpm), $Ph_2PCH_2CH_2PPh_2$ (dpe)) have been synthesized and characterized by electrochemical, infrared, and ^{31}P NMR studies. The electrochemical oxidation of *fac*- and *mer*-$M(CO)_3(\eta^1\text{-P-P})(\eta^2\text{-P-P})$ and the subsequent reduction of the oxidized products at platinum electrodes in acetone and dichloromethane provide substantial thermodynamic, kinetic, and synthetic information on the influence of isomeric form, chelate ring size, and the metal in the formal oxidation states M(0), M(I), and M(II). One-electron oxidation of *mer*-$Cr(CO)_3(\eta^1\text{-dpm})(\eta^2\text{-dpm})$ produces the stable *mer*-$[Cr(CO)_3(\eta^1\text{-dpm})(\eta^2\text{-dpm})]^+$ cation, which on further oxidation produces a highly reactive chromium(II) complex, which is believed to be $[Cr(CO)_3(\eta^2\text{-dpm})_2]^{2+}$. One-electron oxidation of *fac*-$Cr(CO)_3(\eta^1\text{-dpe})(\eta^2\text{-dpe})$ produces the species *fac*-$[Cr(CO)_3(\eta^1\text{-dpe})(\eta^2\text{-dpe})]^+$, which rapidly isomerizes to *mer*-$[Cr(CO)_3(\eta^1\text{-dpe})(\eta^2\text{-dpe})]^+$. Further oxidation of the mer^+ compound leads to complete decomposition. A catalytic process involving a redox cross-reaction or direct electrochemical reduction of *mer*-$[Cr(CO)_3(\eta^1\text{-dpe})(\eta^2\text{-dpe})]^+$ enables the previously unknown *mer*-$Cr(CO)_3(\eta^1\text{-dpe})(\eta^2\text{-dpe})$ to be isolated. Oxidation of *fac*- and *mer*-$M(CO)_3(\eta^1\text{-P-P})(\eta^2\text{-P-P})$ (M = Mo, W) occurs via either two one-electron steps or via a single two-electron step to produce the seven-coordinate $[M(CO)_3(\eta^2\text{-P-P})_2]^{2+}$ cation. The isomeric form of the starting material is important in both thermodynamic and kinetic aspects of the oxidation processes. The stability of the seven-coordinate, 18-electron M(II) complex is far greater than of the chromium analogues. For the dpe complexes the intermediates *mer*-$[M(CO)_3(\eta^1\text{-dpe})(\eta^2\text{-dpe})]^+$ are relatively stable, unlike the case with dpm where rapid disproportionation of the M(I) complex occurs, thus demonstrating the importance of the chelate ring size. Reduction of both the M(I) and M(II) complexes leads exclusively to *mer*-$M(CO)_3(\eta^1\text{-P-P})(\eta^2\text{-P-P})$.

Introduction

The chemical and electrochemical oxidation of 18-electron metal carbonyl complexes has been investigated extensively in the past few years.[3-14] After loss of one or more electrons, the resultant formally 17- or 16-electron species tend to be labile and undergo a wide range of chemical reactions.

In the particular case of complexes *fac*/*mer*-$M(CO)_3P_3$ (M = Cr, Mo; P = monodentate phosphorus ligand) the oxidized species *fac*-$[M(CO)_3P_3]^+$ undergo rapid isomerization to *mer*-$[M(CO)_3P_3]^+$,[11,12] while *mer*-$[M(CO)_3P_3]^+$ species participate in catalytic isomerization reactions[14] and undergo rapid homogeneous electron transfer with their isostructural 18-electron counterparts.[11,12]

If bidentate, or potentially bidentate, phosphorus ligands (P-P) such as bis(diphenylphosphino)methane (dpm) or 1,2-bis(diphenylphosphino)ethane (dpe) are employed instead of monodentate phosphorus ligands to form complexes of the type $M(CO)_3(\eta^1\text{-P-P})(\eta^2\text{-P-P})$, the reaction pathways of the oxidized complexes may become far more varied than for complexes containing exclusively monodentate phosphine ligands, since the η^1-P-P ligand may alter its coordination role after oxidation. If this occurs, then variations in ring size or metal may be expected to be extremely important in determining the thermodynamic and kinetic stability of the oxidized complexes.

In the present paper, the synthesis and characterization of complexes of the type *fac*- and *mer*-$M(CO)_3(\eta^1\text{-P-P})(\eta^2\text{-P-P})$ (M = Cr, Mo, W; P-P = dpm, dpe) are reported, along with a detailed study of the oxidation of these complexes to examine the influence of the bidentate ligands with respect to the chelate ring size and to the metal. During the course of this work, a report describing the electrochemical oxidation of *mer*-$Cr(CO)_3(\eta^1\text{-dpm})(\eta^2\text{-dpm})$ appeared,[13] as well as one describing some chemical reactions of related complexes.[15] However, these studies did not explore the consequences of varying either the ring size of the chelated ligand or the metal nor did they examine the redox properties of the different isomers, which is the purpose of this paper.

Experimental Section

Materials. Chromium, molybdenum, and tungsten hexacarbonyls (Climax Molybdenum Co.; Pressure Chemical Co.) were dried over P_2O_5 and used without further purification. The ligands dpm and dpe (Strem Chemical Co.) were used without further purification. All solvents were either HPLC or AR grade and were dried over molecular sieves.

Preparations. The $M(CO)_3(\eta^1\text{-dpm})(\eta^2\text{-dpm})$ complexes were prepared according to literature methods.[16,17]

***fac*-$Cr(CO)_3(\eta^1\text{-dpe})(\eta^2\text{-dpe})$.** dpe (2.5 mmol) and $(C_7H_8)Cr(CO)_3$ (C_7H_8 = cyclohepta-1,3,5-triene) (1.0 mmol) were refluxed in dichloromethane (30 cm^3) for 4 h under a nitrogen atmosphere. After filtration, *n*-hexane (30 cm^3) was added and the solution chilled overnight at 0 °C to precipitate a pale yellow solid, which was recrystallized from dichloromethane/*n*-hexane (yield: 0.47 g, 56.0%). Attempts to prepare *mer*-$Cr(CO)_3(\eta^1\text{-dpe})(\eta^2\text{-dpe})$ by thermal isomerization of the *fac* isomer failed, but this complex was prepared by techniques based on electrochemical studies as described later in the text.

***fac*-$M(CO)_3(\eta^1\text{-dpe})(\eta^2\text{-dpe})$ (M = Mo, W).** dpe (2.5 mmol) and $(C_7H_8)M(CO)_3$ (M = Mo, W) (1.0 mmol) were dissolved in dichloromethane (30 cm^3) at room temperature. The solution was stirred for 2 h. After filtration, *n*-hexane (30 cm^3) was added and the solution chilled overnight at 0 °C to precipitate an off-white powder. This was recrystallized from dichloromethane/*n*-hexane (yield: M = Mo, 0.63 g, 70.0%; M = W, 0.62 g, 65.2%): mp M = Mo, 196-198 °C; mp M = W, 198-200 °C.

Physical Measurements. Infrared spectra were recorded on a Jasco A-302 spectrometer and were calibrated against polystyrene (1601 cm^{-1}). Phosphorus-31 proton-decoupled NMR spectra were recorded at 40.26 MHz on a JEOL FX 100 spectrometer and referenced against external 85% H_3PO_4. The high-frequency positive convention is used.

---

(1) Deakin University.
(2) University of Melbourne.
(3) Wimmer, F. A.; Snow, M. R.; Bond, A. M. *Inorg. Chem.* **1974**, *13*, 1617.
(4) Bond, A. M.; Colton, R.; Jackowski, J. J. *Inorg. Chem.* **1975**, *14*, 274.
(5) Bond, A. M.; Colton, R. *Inorg. Chem.* **1976**, *15*, 446.
(6) Bond, A. M.; Colton, R. *Inorg. Chem.* **1976**, *15*, 2036.
(7) Bond, A. M.; Colton, R.; McCormick, M. J. *Inorg. Chem.* **1977**, *16*, 155.
(8) Bond, A. M.; Colton, R.; Jackowski, J. J. *Inorg. Chem.* **1979**, *18*, 1977.
(9) Bond, A. M.; Colton, R.; McDonald, M. E. *Inorg. Chem.* **1978**, *17*, 2842.
(10) Bagchi, R. N.; Bond, A. M.; Brain, G.; Colton, R.; Henderson, T. L. E.; Kevekordes, J. E. *Organometallics* **1984**, *3*, 4.
(11) Bond, A. M.; Colton, R.; Carr, S. W. *Organometallics* **1984**, *3*, 541.
(12) Bond, A. M.; Colton, R.; Carr, S. W. *Inorg. Chem.* **1984**, *23*, 2343.
(13) Blagg, A.; Carr, S. W.; Cooper, G. R.; Dobson, I. D.; Gill, J. B.; Goodall, D. C.; Shaw, B. L.; Taylor, N.; Boddington, T. *J. Chem. Soc., Dalton Trans.* **1985**, 1213.
(14) Bond, A. M.; Colton, R.; Kevekordes, J. E. *Inorg. Chem.* **1986**, *25*, 749.
(15) Blagg, A.; Hutton, A. T.; Shaw, B. L.; Thornton-Pett, M. *Inorg. Chim. Acta* **1985**, *100*, L33.
(16) Isaacs, E. E.; Graham, W. A. G. *Inorg. Chem.* **1975**, *14*, 2560.
(17) Blagg, A.; Cooper, G. R.; Pringle, P. G.; Robson, R.; Shaw, B. L. *J. Chem. Soc., Chem. Commun.* **1984**, 933.

0020-1669/86/1325-2378$01.50/0

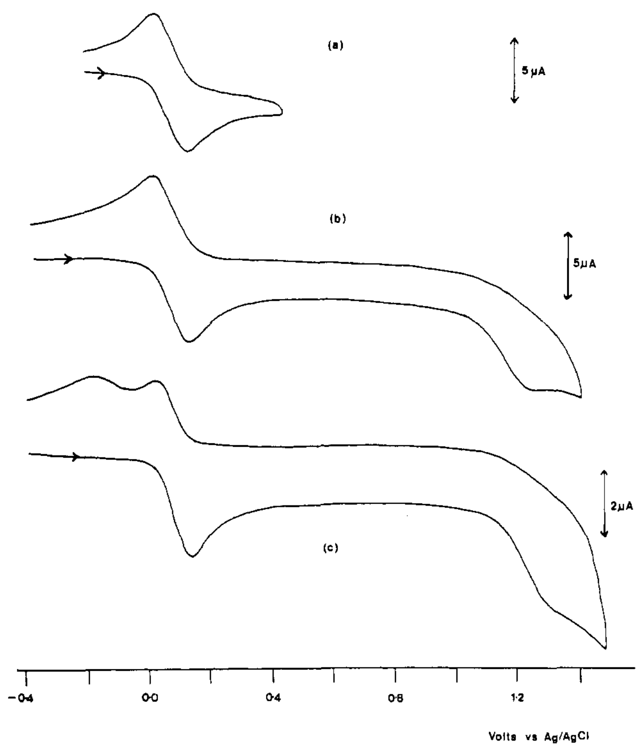

Figure 1. Cyclic voltammograms at a platinum electrode for the oxidation of *mer*-$Cr(CO)_3(\eta^1\text{-dpm})(\eta^2\text{-dpm})$ in CH_2Cl_2 (0.1 M Bu_4NClO_4) with a scan rate of 200 mV s^{-1}: (a) at 20 °C over a restricted voltage range; (b) at 20 °C, including the second oxidation; (c) at −78 °C.

Cyclic voltammograms were recorded in dichloromethane (0.1 M Bu_4NClO_4) and acetone (0.1 M Et_4NClO_4) by using a Model 174 E.G. and G. PAR electrochemistry system. Concentrations of carbonyl compounds for electrochemical studies were in the range 10^{-4}–10^{-3} M. A three-electrode system was used with the working and auxiliary electrodes being platinum wire. The reference electrode was Ag/AgCl (CH_2Cl_2; saturated LiCl) and was separated from the test solution by a salt bridge containing 0.1 M Bu_4NClO_4 in CH_2Cl_2. Frequent calibration of this reference electrode was carried out against a standard ferrocene solution. For variable-temperature cyclic voltammetry the temperature was regulated by using a dry ice/acetone bath and monitored with a thermocouple. Controlled-potential electrolysis experiments were performed with a PAR Model 173 potentiostat/galvanostat using a platinum-gauze working electrode and a platinum auxiliary electrode separated from the bulk solution by a salt bridge containing a Vycor plug. The reference electrode was the same as used in the voltammetric experiments. All solutions were degassed with nitrogen before measurements were taken and were kept under a nitrogen atmosphere during the experiments.

Results and Discussion

Synthesis and Characterization of Complexes. The preparation of *mer*-$Cr(CO)_3(\eta^1\text{-dpm})(\eta^2\text{-dpm})$[13] and the *fac* and *mer* isomers of $Mo(CO)_3(\eta^1\text{-dpm})(\eta^2\text{-dpm})$[16] have been previously reported, and ^{31}P NMR studies show that these complexes contain one monodentate and one bidentate dpm ligand. Similarly, the preparations of *fac*- and *mer*-$W(CO)_3(\eta^1\text{-dpm})(\eta^2\text{-dpm})$ have been reported briefly, although without spectroscopic details.[17]

fac-$W(CO)_3(\eta^1\text{-dpm})(\eta^2\text{-dpm})$ in CH_2Cl_2 solution displays two strong bands in the carbonyl region of the infrared spectrum, consistent with the proposed facial structure, while the *mer* isomer shows two strong bands and one weaker band (Table I). The ^{31}P NMR spectra also clearly distinguish between the isomers (Table II) and are similar to those reported by Isaacs and Graham[16] for the molybdenum analogues. The new complexes *fac*-$M(CO)_3(\eta^1\text{-dpe})(\eta^2\text{-dpe})$ and *mer*-$Cr(CO)_3(\eta^1\text{-dpe})(\eta^2\text{-dpe})$ were characterized by their similar infrared and ^{31}P NMR spectra.

Electrochemical Studies. Electrochemical measurements for the $M(CO)_3(\eta^1\text{-P-P})(\eta^2\text{-P-P})$ complexes were made in dichloromethane and acetone at platinum electrodes, with 0.1 M tetrabutylammonium perchlorate and tetraethylammonium perchlorate as supporting electrolytes, respectively. The electrochemical behavior of each complex was similar in the two solvents, implying that the solvent does not play a dominant role in either thermodynamic or kinetic aspects of the redox reactions, at least on the electrochemical time scale. The electrochemical results are summarized for chromium complexes in Table III and for molybdenum and tungsten complexes in Table IV.

Table I. Infrared Data (cm^{-1}) for the Carbonyl Region in CH_2Cl_2 Solution[a]

fac-$Mo(CO)_3(\eta^1\text{-dpm})(\eta^2\text{-dpm})$	1942 (s)	1845 (s, br)	
fac-$W(CO)_3(\eta^1\text{-dpm})(\eta^2\text{-dpm})$	1938 (s)	1838 (s, br)	
fac-$Cr(CO)_3(\eta^1\text{-dpe})(\eta^2\text{-dpe})$	1928 (s)	1835 (s, br)	
fac-$Mo(CO)_3(\eta^1\text{-dpe})(\eta^2\text{-dpe})$	1938 (s)	1838 (s, br)	
fac-$W(CO)_3(\eta^1\text{-dpe})(\eta^2\text{-dpe})$	1938 (s)	1838 (s, br)	
mer-$Cr(CO)_3(\eta^1\text{-dpm})(\eta^2\text{-dpm})$	1950 (w)	1850 (s)	1830 (sh)
mer-$Mo(CO)_3(\eta^1\text{-dpm})(\eta^2\text{-dpm})$	1970 (w)	1865 (s)	1841 (sh)
mer-$W(CO)_3(\eta^1\text{-dpm})(\eta^2\text{-dpm})$	1959 (w)	1855 (s)	1832 (sh)
mer-$Cr(CO)_3(\eta^1\text{-dpe})(\eta^2\text{-dpe})$	1955 (w)	1850 (s)	1830 (sh)
mer-$[Cr(CO)_3(\eta^1\text{-dpe})(\eta^2\text{-dpe})]^+$	1965 (w)	1910 (s)	1900 (sh)

[a] Key: s, strong; sh, shoulder; br, broad; w, weak.

Table II. Phosphorus-31 NMR Data in Dichloromethane Solution at 20 °C

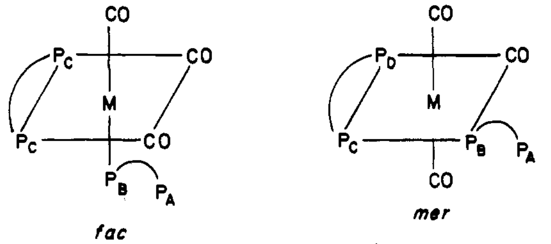

compd	P	δ	$J_{(P\text{-}P)}$, Hz
dpm		−22.7 (s)	
dpe		−13.3 (s)	
fac-$Mo(CO)_3(\eta^1\text{-dpm})(\eta^2\text{-dpm})$	B	28.1 (m)	$J_{(A\text{-}B)} = 34$
	C	1.0 (d)	$J_{(B\text{-}C)} = 27$
	A	−27.3 (d)	
fac-$W(CO)_3(\eta^1\text{-dpm})(\eta^2\text{-dpm})$	B	10.6 (m)	$J_{(B\text{-}C)} = 22$
	C	−22.3 (d)	$J_{(A\text{-}B)} = 34$
	A	−27.3 (d)	
fac-$Cr(CO)_3(\eta^1\text{-dpe})(\eta^2\text{-dpe})$	C	67.9 (d)	$J_{(B\text{-}C)} = 32$
	B	43.5 (m)	$J_{(A\text{-}B)} = 29$
	A	−13.3 (d)	
fac-$Mo(CO)_3(\eta^1\text{-dpe})(\eta^2\text{-dpe})$	C	47.1 (d)	$J_{(B\text{-}C)} = 24$
	B	26.2 (m)	$J_{(A\text{-}B)} = 29$
	A	−13.0 (d)	
fac-$W(CO)_3(\eta^1\text{-dpe})(\eta^2\text{-dpe})$	C	34.2 (d)	$J_{(B\text{-}C)} = 22$
	B	8.2 (m)	$J_{(A\text{-}B)} = 30$
	A	−13.3 (d)	
mer-$Cr(CO)_3(\eta^1\text{-dpm})(\eta^2\text{-dpm})$	B	64.2 (m)	$J_{(A\text{-}B)} = 39$
	C	48.4 (d)	$J_{(B\text{-}C)} = 17$
	D	24.5 (d)	$J_{(B\text{-}D)} = 24$
	A	−26.8 (d)	
mer-$W(CO)_3(\eta^1\text{-dpm})(\eta^2\text{-dpm})$	B	18.5 (t of d)	$J_{(A\text{-}B)} = 61$
	D	−12.5 (d of d)	$J_{(B\text{-}C)} = 30$
	C	−25.3 (t)	$J_{(B\text{-}D)} = 69$
	A	−26.6 (d)	$J_{(C\text{-}D)} = 30$
mer-$Cr(CO)_3(\eta^1\text{-dpe})(\eta^2\text{-dpe})$[b]	C	92.6 (br)	$J_{(A\text{-}B)} = 23$
	B	74.7 (br)	$J_{(B\text{-}D)} = 35$
	D	30.8 (d)	
	A	−13.3 (d)	

[a] Key: s, singlet; d, doublet; t, triplet; m, multiplet; br, broad.
[b] Resonances due to P_C and P_B are broad, probably due to fast electron exchange with a small amount of *mer*-$[Cr(CO)_3(^1\eta\text{-dpe})(\eta^2\text{-dpe})]^+$, which is almost inevitably present due to the method of preparation. As a result, fine structure on these peaks is not resolved and the assignment of their identities may be reversed.

(i) *mer*-$Cr(CO)_3(\eta^1\text{-dpm})(\eta^2\text{-dpm})$. The cyclic voltammogram of *mer*-$Cr(CO)_3(\eta^1\text{-dpm})(\eta^2\text{-dpm})$ at 20 °C exhibits a chemically reversible one-electron-redox couple (scan rate 50–500 mV s^{-1}) at low positive potential vs. Ag/AgCl in both dichloromethane and acetone as reported by Shaw et al.[13] (Table III and Figure 1a). This redox couple is similar in electrochemical characteristics

Table III. Electrochemical Data for $Cr(CO)_3(\eta^1\text{-P-P})(\eta^2\text{-P-P})$ Systems for Approximately 10^{-3} M Solutions[a]

compd	solvent	E_p^{ox},[b] V	E_p^{red},[b] V	$E°$,[b,c] V	T, °C
mer-$Cr(CO)_3(\eta^1\text{-dpm})(\eta^2\text{-dpm})$	CH_2Cl_2	0.15	0.02	0.09	20
	acetone	0.08	−0.00	0.04	20
mer-$[Cr(CO)_3(\eta^1\text{-dpm})(\eta^2\text{-dpm})]^+$	CH_2Cl_2	1.27			20
	acetone	1.00			20
$[Cr(CO)_3(\eta^2\text{-dpm})_2]^{2+}$	CH_2Cl_2		−0.16		−78
fac-$Cr(CO)_3(\eta^1\text{-dpe})(\eta^2\text{-dpe})$	CH_2Cl_2	0.43			20
	CH_2Cl_2	0.47	0.38	0.43	−78
	acetone	0.37			20
mer-$Cr(CO)_3(\eta^1\text{-dpe})(\eta^2\text{-dpe})$	CH_2Cl_2	0.22	0.13	0.18	20
	acetone	0.18	0.10	0.14	20
mer-$[Cr(CO)_3(\eta^1\text{-dpe})(\eta^2\text{-dpe})]^+$	CH_2Cl_2	1.24			20
	acetone	1.11			20

[a] The $E_{1/2}^r$ ($\simeq E°$) values for the ferrocenium/ferrocene couple are 0.50 (CH_2Cl_2) and 0.42 V (acetone) vs. Ag/AgCl. [b] Vs. Ag/AgCl. [c] The standard redox potential $E°$ was calculated on the basis of theoretical studies using digital simulation of the quasi-reversible electrode process, assuming equal diffusion coefficients for oxidized and reduced species. In practice these values were the same as the mean of E_p^{ox} and E_p^{red}.

Table IV. Electrochemical Data for the $M(CO)_3(\eta^1\text{-P-P})(\eta^2\text{-P-P})$ Complexes (M = Mo, W) at 20 °C[a]

compd	solvent	E_p^{ox},[b] V	E_p^{red},[b] V	$E°$,[b] V
mer-$Mo(CO)_3(\eta^1\text{-dpm})(\eta^2\text{-dpm})$	CH_2Cl_2	0.42		
	acetone	0.24		
fac-$Mo(CO)_3(\eta^1\text{-dpm})(\eta^2\text{-dpm})$	CH_2Cl_2	0.68		
	acetone	0.52		
$[Mo(CO)_3(\eta^2\text{-dpm})_2]^{2+}$	CH_2Cl_2		−0.35	
	acetone		−0.32	
fac-$W(CO)_3(\eta^1\text{-dpm})(\eta^2\text{-dpm})$	CH_2Cl_2	0.59		
	acetone	0.50		
mer-$W(CO)_3(\eta^1\text{-dpm})(\eta^2\text{-dpm})$	CH_2Cl_2	0.34		
	acetone	0.23		
$[W(CO)_3(\eta^2\text{-dpm})_2]^{2+}$	CH_2Cl_2		−0.43	
	acetone		−0.47	
fac-$Mo(CO)_3(\eta^1\text{-dpe})(\eta^2\text{-dpe})$	CH_2Cl_2	0.61		
mer-$Mo(CO)_3(\eta^1\text{-dpe})(\eta^2\text{-dpe})$	CH_2Cl_2	0.45	0.35	0.40
mer-$[Mo(CO)_3(\eta^1\text{-dpe})(\eta^2\text{-dpe})]^+$	CH_2Cl_2	1.10		
$[Mo(CO)_3(\eta^2\text{-dpe})_2]^{2+}$	CH_2Cl_2		−0.46	
fac-$W(CO)_3(\eta^1\text{-dpe})(\eta^2\text{-dpe})$	CH_2Cl_2	0.58		
mer-$W(CO)_3(\eta^1\text{-dpe})(\eta^2\text{-dpe})$	CH_2Cl_2	0.46	0.36	0.41
mer-$[W(CO)_3(\eta^1\text{-dpe})(\eta^2\text{-dpe})]^+$	CH_2Cl_2	1.16		
$[W(CO)_3(\eta^2\text{-dpe})_2]^{2+}$	CH_2Cl_2		−0.60	

[a] Calibration against ferrocene as for Table III. [b] Vs. Ag/AgCl.

to the known one-electron chemically and electrochemically reversible oxidation of ferrocene and may be assigned as a *mer*$^{+/0}$ redox couple:[13]

$$mer\text{-}Cr(CO)_3(\eta^1\text{-dpm})(\eta^2\text{-dpm}) \rightleftarrows mer\text{-}[Cr(CO)_3(\eta^1\text{-dpm})(\eta^2\text{-dpm})]^+ + e^- \quad (1)$$

Such behavior is characteristic of the *mer*^{0} tricarbonyl complexes previously studied.[7,9,11,12] The electrochemistry of this process remains chemically reversible at −78 °C and unchanged after repeated scans.

At more positive potentials a second one-electron-oxidation process is observed close to the solvent limit (Figure 1b). This process involves the oxidation of *mer*-$[Cr(CO)_3(\eta^1\text{-dpm})(\eta^2\text{-dpm})]^+$ and the subsequent decomposition of the product at room temperature as shown in eq 2, (no carbonyl stretch for the final

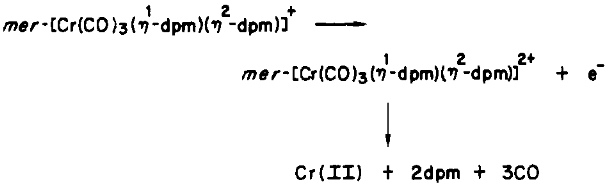

$$\begin{array}{l} mer\text{-}[Cr(CO)_3(\eta^1\text{-dpm})(\eta^2\text{-dpm})]^+ \longrightarrow \\ \qquad mer\text{-}[Cr(CO)_3(\eta^1\text{-dpm})(\eta^2\text{-dpm})]^{2+} + e^- \\ \qquad \qquad \downarrow \\ \qquad Cr(II) + 2dpm + 3CO \end{array} \quad (2)$$

product). No additional reduction process was observed on the reverse scans of cyclic voltammograms at ambient temperature. However at −78 °C, while the second oxidation process remains irreversible, a new irreversible reduction wave appears on the reverse scan with a peak potential E_p^{red} of −0.16 V (Figure 1c), which does not appear when the potential is switched before the second oxidation is reached. This implies that the reduction process observed at −0.16 V at −78 °C results from a species produced in the second oxidation step and that probably a Cr(II) carbonyl species formed during this oxidation has some stability on the electrochemical time scale, although only at low temperatures. (See later data on the molybdenum and tungsten complexes for identification of this product.)

Controlled-potential oxidative electrolysis of *mer*-$Cr(CO)_3(\eta^1\text{-dpm})(\eta^2\text{-dpm})$ in acetone at 0.6 V vs. Ag/AgCl at 20 °C confirms that 1.0 ± 0.1 electron is transferred during the first oxidation step. The reductive cyclic voltammogram of this oxidized solution exhibited a quasi-reversible one-electron reduction, where the positions of E_p^{red} and E_p^{ox} were coincident with those observed for the oxidation of *mer*-$Cr(CO)_3(\eta^1\text{-dpm})(\eta^2\text{-dpm})$ in acetone. Therefore the species formed on oxidation of *mer*-$Cr(CO)_3(\eta^1\text{-dpm})(\eta^2\text{-dpm})$ is *mer*-$[Cr(CO)_3(\eta^1\text{-dpm})(\eta^2\text{-dpm})]^+$. The second irreversible oxidation wave at 1.00 V in acetone remains after controlled-potential oxidative electrolysis of *mer*-$Cr(CO)_3(\eta^1\text{-dpm})(\eta^2\text{-dpm})$ at 0.60 V as required by the proposed mechanism, and this wave corresponds to eq 2. *mer*-$[Cr(CO)_3(\eta^1\text{-dpm})(\eta_2\text{-dpm})]^+$ in acetone can be quantitatively converted back to the starting material via reductive controlled-potential electrolysis at −0.6 V vs. Ag/AgCl as required for the proposed mechanism.

The reversible behavior of the *mer*$^{+/0}$ redox couple indicates that the 17-electron *mer*$^+$ species is stable on the coulometric time scale ($\simeq$30 min) in acetone and that chemical oxidation and isolation of the Cr(I) species is possible. In our work we can find no evidence for the disproportionation of the *mer*$^+$ species on the electrochemical time scale as claimed by Shaw et al.[13] Furthermore, the reaction

$$mer\text{-}[Cr(CO)_3(\eta^1\text{-dpm})(\eta^2\text{-dpm})]^+ \rightarrow trans\text{-}[Cr(CO)_2(\eta^2\text{-dpm})_2]^+ + CO \quad (3)$$

discussed by these authors certainly does occur on the longer time scale, but it does not influence data on the electrochemical time scale.

(ii) *fac*-$Cr(CO)_3(\eta^1\text{-dpe})(\eta^2\text{-dpe})$. The cyclic voltammogram for the new compound *fac*-$Cr(CO)_3(\eta^1\text{-dpe})(\eta^2\text{-dpe})$ in dichloromethane at 20 °C is shown in Figure 2a. On the first scan an oxidation wave with a peak potential E_p^{ox} of 0.43 V is observed, but no corresponding reduction peak appeared on the reverse scan (scan rate = 200 mV s^{-1}). However a reduction wave is observed with an E_p^{red} value of 0.13 V, and on second and subsequent scans the other half of this quasi-reversible couple appears with E_p^{ox} at 0.22 V. The irreversible process occurring at 0.43 V may be assigned as:

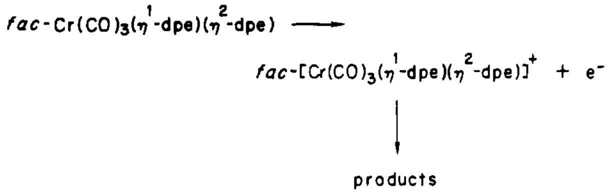

$$\begin{array}{l} fac\text{-}Cr(CO)_3(\eta^1\text{-dpe})(\eta^2\text{-dpe}) \longrightarrow \\ \qquad fac\text{-}[Cr(CO)_3(\eta^1\text{-dpe})(\eta^2\text{-dpe})]^+ + e^- \\ \qquad \qquad \downarrow \\ \qquad \qquad products \end{array} \quad (4)$$

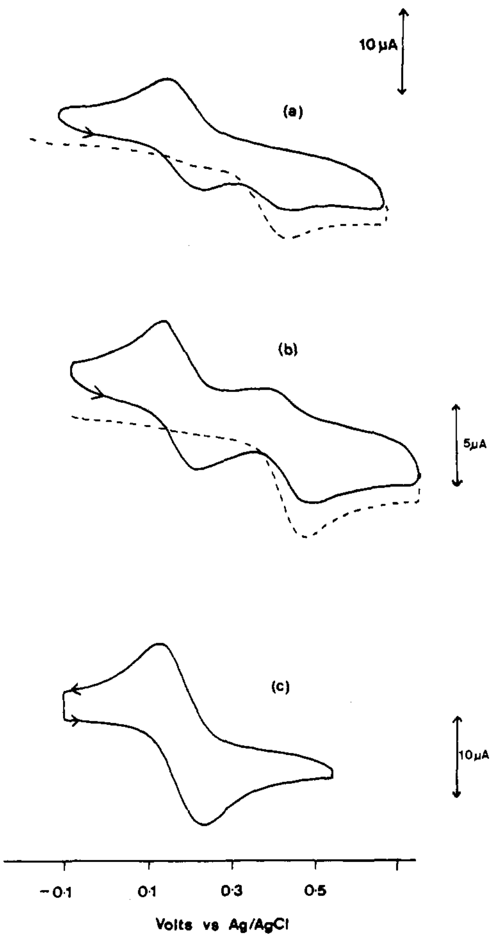

Figure 2. Cyclic voltammograms at a platinum electrode for the $Cr(CO)_3(\eta^1\text{-dpe})(\eta^2\text{-dpe})$ system in CH_2Cl_2 (0.1 M Bu_4NClO_4) with a scan rate of 200 mV s^{-1} [(---) first scans; (—) second scans]: (a) for a freshly prepared solution of *fac*-$Cr(CO)_3(\eta^1\text{-dpe})(\eta^2\text{-dpe})$ at 20 °C; (b) for a freshly prepared solution of *fac*-$Cr(CO)_3(\eta^1\text{-dpe})(\eta^2\text{-dpe})$ at −78 °C; (c) for a solution about 30 min after the initial cyclic voltammogram at 20 °C.

That is, *fac*-$[Cr(CO)_3(\eta^1\text{-dpe})(\eta^2\text{-dpe})]^+$ is unstable on the electrochemical time scale at 20 °C and decomposes to a new species, which shows a quasi-reversible couple at less positive potentials ($E_{1/2}{}^r \simeq E° = 0.18$ V). Previous results for dicarbonyl[3,4] and tricarbonyl[7,9,11,12] systems suggest that isomerization of *fac*$^+$ to *mer*$^+$ has occurred and that the new peaks are due to the *mer*$^{+/0}$ redox couple. This interpretation is confirmed by the preparation, characterization, and electrochemistry of both *mer*-$Cr(CO)_3(\eta^1\text{-dpe})(\eta^2\text{-dpe})$ and *mer*-$[Cr(CO)_3(\eta^1\text{-dpe})(\eta^2\text{-dpe})]^+$ (see below).

At −78 °C the cyclic voltammogram of *fac*-$Cr(CO)_3(\eta^1\text{-dpe})(\eta^2\text{-dpe})$ (Figure 2b) provides direct evidence for the formation of *fac*-$[Cr(CO)_3(\eta^1\text{-dpe})(\eta^2\text{-dpe})]^+$. Fac$^+$ is more stable on the electrochemical time scale at this temperature, existing for sufficient time to show some reduction to *fac*^{0} on the reverse scan. At more positive potentials, a second irreversible oxidation wave is observed at 1.24 V. This wave appears at +20 and −78 °C at the same potential; however, on the reverse scan no new reduction process is seen at either temperature, differing in temperature dependence from the behavior of the second oxidation wave observed for *mer*-$Cr(CO)_3(\eta^1\text{-dpm})(\eta^2\text{-dpm})$. This wave will be discussed in more detail later.

Controlled-potential electrolysis of *fac*-$Cr(CO)_3(\eta^1\text{-dpe})(\eta^2\text{-dpe})$ at 0.6 V in acetone at room temperature confirms that the first oxidation process involves a single electron transfer. The reductive cyclic voltammogram of the resulting Cr(I) species exhibits a quasi-reversible one-electron-reduction wave with the potentials $E_p{}^{red}$ and $E_p{}^{ox}$ coincident with those for the *mer*$^{+/0}$ redox couple in acetone. A second irreversible oxidation wave at (1.11 V in acetone) is again observed when scanning in the positive direction from 0.6 V, corresponding to the oxidation of *mer*-$[Cr(CO)_3(\eta^1\text{-dpe})(\eta^2\text{-dpe})]^+$.

There was no evidence at 20 °C for any *mer*^{0} compound on the first oxidative scan of a freshly prepared solution of *fac*-$Cr(CO)_3(\eta^1\text{-dpe})(\eta^2\text{-dpe})$ in dichloromethane. However, after several cyclic voltammograms had been performed on the same solution, a small oxidation peak corresponding to the oxidation of the *mer*^{0} isomer to *mer*$^+$ was observed on subsequent scans. After some time (≃30 min) at 20 °C, cyclic voltammograms of the same solution revealed the presence of only a small amount of the *fac*^{0} isomer, with the bulk of the complex then being in the form of the *mer*^{0} isomer (Figure 2c). Experiments repeated in acetone gave similar results. In contrast, ^{31}P NMR monitoring over several hours of a freshly prepared solution of *fac*-$Cr(CO)_3(\eta^1\text{-dpe})(\eta^2\text{-dpe})$ in CH_2Cl_2 (with and without added supporting electrolyte Bu_4NClO_4) gave no evidence for isomerization. Therefore, the isomerization after electrochemical oxidation, described above, depends on the presence of a small amount of oxidized species and must involve electron transfer catalysis. After oxidation of *fac*^{0} to *fac*$^+$, isomerization occurs to generate the *mer*$^+$ species, which is the electronically and sterically preferred 17-electron species.[18] Under these conditions *mer*^{0} may be produced via the redox cross-reaction

$$\begin{aligned} &fac\text{-}Cr(CO)_3(\eta^1\text{-dpe})(\eta^2\text{-dpe}) + \\ &\qquad mer\text{-}[Cr(CO)_3(\eta^1\text{-dpe})(\eta^2\text{-dpe})]^+ \overset{K}{\rightleftharpoons} \\ &\qquad fac\text{-}[Cr(CO)_3(\eta^1\text{-dpe})(\eta^2\text{-dpe})]^+ + \\ &\qquad\qquad mer\text{-}Cr(CO)_3(\eta^1\text{-dpe})(\eta^2\text{-dpe}) \quad (5) \end{aligned}$$

even though this reaction is not favored thermodynamically. The resulting *fac*$^+$ rapidly isomerizes to *mer*$^+$, thus repeating the cycle, until the final result is complete isomerization of *fac*^{0} to *mer*^{0} via electron-transfer catalysis.

(iii) *mer*-$[Cr(CO)_3(\eta^1\text{-dpe})(\eta^2\text{-dpe})]^{+/0}$. The electrochemical studies described above indicate that *mer*-$Cr(CO)_3(\eta^1\text{-dpe})(\eta^2\text{-dpe})$ and *mer*-$[Cr(CO)_3(\eta^1\text{-dpe})(\eta^2\text{-dpe})]^+$ have some stability on both the electrochemical and synthetic time scales, and thus the difficulties associated with the preparation of the *mer*^{0} isomer by more usual methods (see Experimental Section) appear to be governed by kinetic factors, rather than any lack of stability of the compound.

Controlled-potential electrolysis or chemical oxidation ($NOPF_6$), of *fac*-$Cr(CO)_3(\eta^1\text{-dpe})(\eta^2\text{-dpe})$ in acetone led to the isolation of *mer*-$[Cr(CO)_3(\eta^1\text{-dpe})(\eta^2\text{-dpe})]^+$; the complex is less stable in dichloromethane on the synthetic time scale. The paramagnetic cation was identified by infrared spectroscopy, and data are given in Table I. A solution of *mer*-$[Cr(CO)_3(\eta^1\text{-dpe})(\eta^2\text{-dpe})]^+$ in dichloromethane gave a reductive cyclic voltammogram that showed a quasi-reversible couple with $E_p{}^{red} = 0.13$ V and $E_p{}^{ox} = 0.22$ V (scan rate = 200 mV s^{-1}) corresponding exactly with the peaks described earlier in the discussion of the electrochemistry associated with *fac*-$Cr(CO)_3(\eta^1\text{-dpe})$ $(\eta^2\text{-dpe})$, thus confirming that *mer*-$[Cr(CO)_3(\eta^1\text{-dpe})(\eta^2\text{-dpe})]^+$ is formed by isomerization of the *fac*$^+$ species.

Controlled-potential reduction of *mer*-$[Cr(CO)_3(\eta^1\text{-dpe})(\eta^2\text{-dpe})]^+$ in acetone at −0.6 V gives *mer*-$Cr(CO)_3(\eta^1\text{-dpe})(\eta^2\text{-dpe})$. This complex may also be conveniently generated by utilizing the catalytic scheme represented in eq 5 by addition of a very small amount of oxidant such as $NOPF_6$ to *fac*-$Cr(CO)_3(\eta^1\text{-dpe})(\eta^2\text{-dpe})$ in dichloromethane. The reaction was monitored by infrared spectroscopy, and after a few minutes the complex was entirely in the *mer*^{0} form. An oxidative cyclic voltammogram of this solution gave the same quasi-reversible couple noted above, together with a second irreversible oxidation at 1.24 V, previously noted in the oxidation of *fac*-$Cr(CO)_3(\eta^1\text{-dpe})(\eta^2\text{-dpe})$, which is due to further oxidation of *mer*-$[Cr(CO)_3(\eta^1\text{-dpe})(\eta^2\text{-dpe})]^+$ in a manner analogous to eq 2.

(iv) *mer*-$Mo(CO)_3(\eta^1\text{-dpm})(\eta^2\text{-dpm})$. The electrochemical behavior of *mer*-$Mo(CO)_3(\eta^1\text{-dpm})(\eta^2\text{-dpm})$ is quite different from

---

(18) Mingos, D. M. P. *J. Organomet. Chem.* **1979**, *C29*, 179.

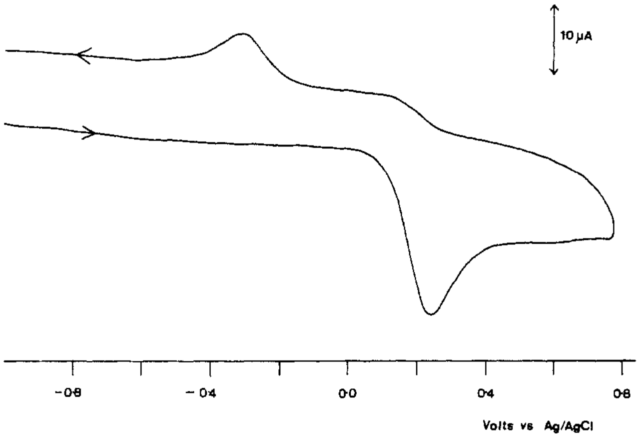

Figure 3. Cyclic voltammogram at a platinum electrode for the oxidation of *mer*-Mo(CO)$_3$(η^1-dpm)(η^2-dpm) in acetone (0.1 M Et$_4$NClO$_4$) at 20 °C and with a scan rate of 200 mV s^{-1}.

that observed for all other group VI (group 6[27]) meridional tricarbonyl complexes previously studied.[7,9,11,12] In contrast to these complexes, which all display quasi-reversible one-electron couples that can be assigned to the *mer*$^{+/0}$ couple, the cyclic voltammogram for *mer*-Mo(CO)$_3$(η^1-dpm)(η^2-dpm) in acetone (Table IV and Figure 3) exhibits an electrochemically irreversible oxidation (E_p^{ox} = 0.24 V) on the first positive scan (scan rate = 200 mV s^{-1}) and an electrochemically irreversible reduction (E_p^{red} = −0.32 V) on the reverse scan. No second oxidation wave is observed at more positive potentials, unlike for the chromium dpm and dpe complexes discussed earlier. The electrochemical behavior of *mer*-Mo(CO)$_3$(η^1-dpm)(η^2-dpm) was unchanged at −78 °C nor did it vary with respect to chemical reversibility over a wide range of scan rates. The oxidation process at 0.24 V may be assigned to the oxidation of the *mer*^{0} complex. The absence of a corresponding reduction wave at a similar potential on the reverse scan indicates that the product of oxidation is also unstable on the electrochemical time scale, and rearranges or decomposes to a new species, which gives the irreversible reduction peak at −0.32 V. The product of this reduction is also unstable on the short time scale, since no corresponding oxidation is observed at a similar potential on the subsequent oxidation scan. Repeated scans show no new features nor is there any signficant depletion of the peak due to the oxidation of the *mer*^{0} complex.

Oxidative controlled-potential electrolysis at 0.8 V of *mer*-Mo(CO)$_3$(η^1-dpm)(η^2-dpm) in acetone demonstrates that two electrons are transferred during oxidation. Reductive cyclic voltammetry of the Mo(II) species formed as a result of the oxidation shows an irreversible reduction at −0.32 V on the first scan, due to the reduction of the Mo(II) species, and an irreversible oxidation at 0.24 V on the reverse scan. The product of the two-electron oxidation is not stable, and when the product is left standing, the peak height of the reduction process at −0.32 V decreases with time. The positions of these responses are exactly the same as those shown in Figure 3 and indicate that *mer*-Mo(CO)$_3$(η^1-dpm)(η^2-dpm) is the product of the reduction of the Mo(II) species. This was confirmed by a reductive controlled-potential electrolysis of a solution of the Mo(II) compound (generated electrochemically as above) at −0.5 V, which showed that two electrons were transferred in the reduction, and in addition, an oxidative cyclic voltammogram of the reduced solution was identical in every respect to that of a solution of *mer*-Mo(CO)$_3$(η^1-dpm)(η^2-dpm). Thus *mer*-Mo(CO)$_3$(η^1-dpm)(η^2-dpm) and the Mo(II) species giving the reduction response at −0.32 V are electrochemically interchangable although the oxidation and reduction do not constitute an electrochemically reversible couple within the usual meaning of the term.

(v) *fac*-Mo(CO)$_3$(η^1-dpm)(η^2-dpm). The electrochemical behavior of *fac*-Mo(CO)$_3$(η^1-dpm)(η^2-dpm) is also quite unlike that of other group VI facial tricarbonyl species examined previously. In contrast *fac*-Cr(CO)$_3$(η^1-dpe)(η^2-dpe), described above, is a typical example. On the first scan, an oxidative cyclic voltammogram for *fac*-Mo(CO)$_3$(η^1-dpm)(η^2-dpm) in acetone at 20 °C (Table IV and Figure 4a) at a scan rate of 200 mV s^{-1} exhibits an electrochemically irreversible oxidation wave at 0.52 V and an electrochemically irreversible reduction wave at −0.32 V on the reverse scan. On second and subsequent scans (Figure 4, parts b and c) a second irreversible oxidation wave appears at 0.24 V, which increases in height at the expense of the oxidation peak at 0.52 V as the number of scans increases. However, if cyclic voltammograms are restricted to the potential range 0.1–0.8 V (Figure 4d), then repetitive scanning shows only the irreversible oxidation wave at 0.52 V and the second oxidation wave at 0.24 V does not appear. This implies that the appearance of the wave at 0.24 V is a result of the reduction process at −0.32 V.

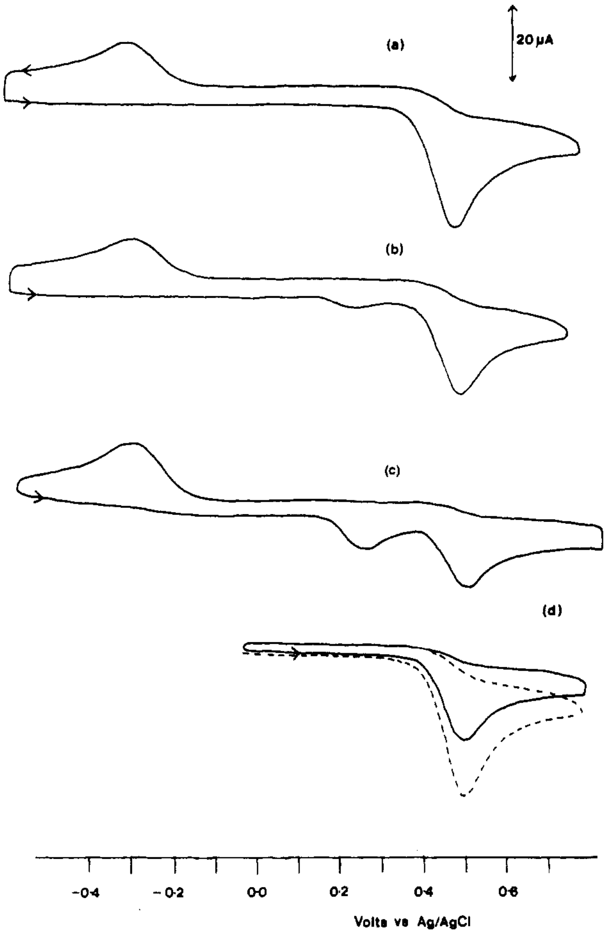

Figure 4. Cyclic voltammograms at a platinum electrode for the oxidation of *fac*-Mo(CO)$_3$(η^1-dpm)(η^2-dpm) in acetone (0.1 M Et$_4$NClO$_4$) at 20 °C, and with a scan rate of 200 mV s^{-1}: (a) first scan, (b) second scan, (c) fifth scan, (d) first (- - -) and subsequent (—) scans over a restricted potential range.

The irreversible oxidation at 0.52 V may be assigned to the oxidation of the *fac*-Mo(CO)$_3$(η^1-dpm)(η^2-dpm) complex. Comparison between Figures 3 and 4 shows that the oxidation at 0.24 V and the reduction at −0.32 V are the same as those discussed above for the *mer*-Mo(CO)$_3$(η^1-dpm)(η^2-dpm) system; that is, *mer*^{0} and the same Mo(II) complex are formed after electrochemical oxidation and reduction cycles irrespective of the isomeric form of the starting material. Oxidative controlled-potential electrolysis of *fac*-Mo(CO)$_3$(η^1-dpm)(η^2-dpm) at 0.8 V confirms that two electrons are transferred in the oxidation. A reductive cyclic voltammogram of the oxidized species exhibits the same responses as one produced by oxidation of *mer*-Mo(CO)$_3$(η^1-dpm)(η^2-dpm).

The Mo(II) species generated by the oxidation of both *fac*- and *mer*-Mo(CO)$_3$(η^1-dpm)(η^2-dpm) has not yet been isolated and characterized as it is a reactive species. However, it must retain three carbonyl groups and both dpm ligands in order to produce the chemically reversible oxidation and reduction steps. Many seven-coordinate Mo(II) and W(II) carbonyl complexes are known,[19-26] and we suggest that the 16-electron species [Mo-

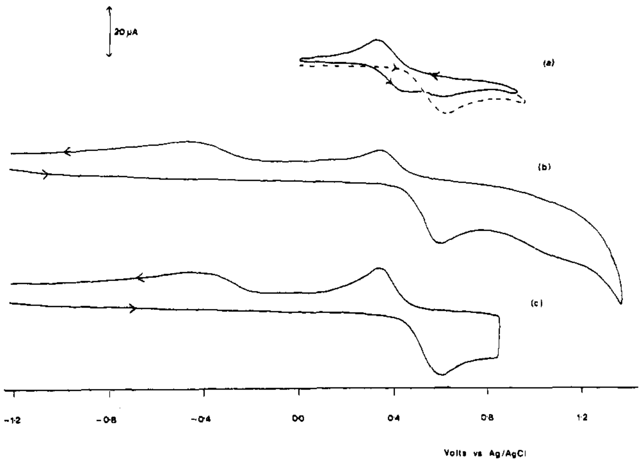

Figure 5. Cyclic voltammograms at a platinum electrode for the oxidation of *fac*-$Mo(CO)_3(\eta^1\text{-dpe})(\eta^2\text{-dpe})$ in CH_2Cl_2 (0.1 M Bu_4NClO_4) at 20 °C and with a scan rate of 200 mV s^{-1}: (a) over a restricted potential range with the direction switched just after the first oxidation [(---) first scan, (—) second scan]; (b) over a wider potential range including the second oxidation; (c) over a restricted potential range but with the potential held at 0.81 V vs. Ag/AgCl for $\simeq$30 s.

$(CO)_3(\eta^1\text{-dpm})(\eta^2\text{-dpm})]^{2+}$ formed on oxidation of either *fac*- or *mer*-$Mo(CO)_3(\eta^1\text{-dpm})(\eta^2\text{-dpm})$ rearranges very rapidly to give the 18-electron, seven-coordinate $[Mo(CO)_3(\eta^2\text{-dpm})_2]^{2+}$ cation. This explains why the oxidation is not electrochemically reversible. On the reverse scan $[Mo(CO)_3(\eta^2\text{-dpm})_2]^{2+}$ is reduced at -0.32 V; reduction of an 18-electron carbonyl complex usually proceeds by two-electron transfer and loss of a ligand to give another 18-electron complex with a reduction of one in the coordination number. In this particular case, a ligand is not completely lost, but one of the dpm ligands reverts to monodentate coordination, generating *mer*-$Mo(CO)_3(\eta^1\text{-dpm})(\eta^2\text{-dpm})$. Further insight into the oxidation process generating the Mo(II) species is gleaned from the corresponding dpe systems described below.

It is assumed that the analogous $[Cr(CO)_3(\eta^2\text{-dpm})_2]^{2+}$ is responsible for the reduction wave at -0.16 V at -78 °C described in section i. However, in this case the seven-coordinate complex is observed only on short time scale experiments at low temperature, implying very limited stability. This is consistent with the generally much lower stability of seven-coordinate Cr(II) complexes compared with their molybdenum and tungsten analogues.

(vi) *fac*- and *mer*-$W(CO)_3(\eta^1\text{-dpm})(\eta^2\text{-dpm})$. The electrochemical behavior of these complexes is very similar to that displayed by their molybdenum analogues. All data are given in Table IV.

(vii) *fac*-$Mo(CO)_3(\eta^1\text{-dpe})(\eta^2\text{-dpe})$. This system provides an interesting type of behavior intermediate between that normally expected for facial tricarbonyl complexes, as exemplified by *fac*-$Cr(CO)_3(\eta^1\text{-dpe})(\eta^2\text{-dpe})$ described earlier, and the highly unusual behavior of *fac*-$Mo(CO)_3(\eta^1\text{-dpm})(\eta^2\text{-dpm})$ described above.

Oxidative cyclic voltammograms for *fac*-$Mo(CO)_3(\eta^1\text{-dpe})(\eta^2\text{-dpe})$ in dichloromethane up to a potential of 1.0 V vs. Ag/AgCl show typical facial isomer behavior; on the first scan (scan rate = 200 mV s^{-1}) there is an electrochemically irreversible oxidation ($E_p^{ox} = 0.61$ V) and on the reverse scan a reduction is observed at 0.35 V. On the second and subsequent scans an oxidation at 0.45 V is also observed in addition to the original process at 0.61 V (Table IV and Figure 5a). The electrochemical response is similar at -78 °C. The interpretation of this data is similar to that for other *fac* tricarbonyl systems, that is, *fac*-$[Mo(CO)_3(\eta^1\text{-dpe})(\eta^2\text{-dpe})]^+$, initially formed on oxidation, is unstable at both room temperature and at -78 °C and it rapidly isomerizes to *mer*-$[Mo(CO)_3(\eta^1\text{-dpe})(\eta^2\text{-dpe})]^+$, which may be reversibly reduced to *mer*-$Mo(CO)_3(\eta^1\text{-dpe})(\eta^2\text{-dpe})$.

If the potential range for the oxidative cyclic voltammogram for *fac*-$Mo(CO)_3(\eta^1\text{-dpe})(\eta^2\text{-dpe})$ is increased, a second electrochemically irreversible oxidation is observed at 1.10 V (Figure 5b), and on the reverse scan a new electrochemically irreversible reduction appears at -0.46 V, in addition to the features described earlier. These additional peaks are similar to those observed in the $Mo(CO)_3(dpm)_2$ system, and the interpretation is similar; that is, a two-electron oxidation of *fac*- or *mer*-$Mo(CO)_3(\eta^1\text{-dpe})(\eta^2\text{-dpe})$ gives $[Mo(CO)_3(\eta^2\text{-dpe})_2]^{2+}$, which in turn is reduced to *mer*-$Mo(CO)_3(\eta^1\text{-dpe})(\eta^2\text{-dpe})$ at -0.46 V. An important difference between the dpm and dpe systems however is that, for dpe, Mo(I) is seen as a relatively stable intermediate, and this provides some further information on the redox process that generates Mo(II). If, after the first oxidation wave at 0.61 V, the potential is held at 0.8 V for $\simeq$15–30 s and then reversed without proceeding to 1.10 V, the reverse scan then exhibits a weak reduction process at -0.46 V (Figure 5c). This wave at -0.46 V corresponds to the reduction of the $[Mo(CO)_3(\eta^2\text{-dpe})_2]^{2+}$, as seen previously. Thus, $[Mo(CO)_3(\eta^2\text{-dpe})_2]^{2+}$ may be generated by direct oxidation of *mer*-$[Mo(CO)_3(\eta^1\text{-dpe})(\eta^2\text{-dpe})]^+$ at 1.10 V or formed from this compound with time at a lower potential. This implies that some type of disproportionation mechanism is involved with the latter pathway, as seen in earlier studies of group VI metal carbonyl systems:[5]

$$2\,mer\text{-}[Mo(CO)_3(\eta^1\text{-dpe})(\eta^2\text{-dpe})]^+ \rightarrow mer\text{-}Mo(CO)_3(\eta^1\text{-dpe})(\eta^2\text{-dpe}) + mer\text{-}[Mo(CO)_3(\eta^1\text{-dpe})(\eta^2\text{-dpe})]^{2+}$$

$$mer\text{-}[Mo(CO)_3(\eta^1\text{-dpe})(\eta^2\text{-dpe})]^{2+} \rightarrow [Mo(CO)_3(\eta^2\text{-dpe})_2]^{2+} \quad (6)$$

Alternatively

$$\begin{tikzcd}
fac\text{-}Mo(CO)_3(\eta^1\text{-dpe})(\eta^2\text{-dpe}) \arrow[r] & fac\text{-}[Mo(CO)_3(\eta^1\text{-dpe})(\eta^2\text{-dpe})]^+ + e^- \arrow[d] \\
\text{or} & \\
mer\text{-}Mo(CO)_3(\eta^1\text{-dpe})(\eta^2\text{-dpe}) \arrow[r] & mer\text{-}[Mo(CO)_3(\eta^1\text{-dpe})(\eta^2\text{-dpe})]^+ \arrow[d] \\
& mer\text{-}[Mo(CO)_3(\eta^1\text{-dpe})(\eta^2\text{-dpe})]^{2+} + e^- \arrow[d] \\
& [Mo(CO)_3(\eta^2\text{-dpe})_2]^{2+} \quad (7)
\end{tikzcd}$$

(viii) *fac*-$W(CO)_3(\eta^1\text{-dpe})(\eta^2\text{-dpe})$. The electrode processes for *fac*-$W(CO)_3(\eta^1\text{-dpe})(\eta^2\text{-dpe})$ are similar to those described for the molybdenum analogue, and the electrochemical data are presented in Table IV.

General Discussion. The electrochemical behavior of the $M(CO)_3(P\text{-}P)_2$ complexes involves several processes and the identity of the metal and of the ditertiary phosphine affects the observed electrochemistry.

fac-$M(CO)_3(\eta^1\text{-dpe})(\eta^2\text{-dpe})$ and *mer*-$Cr(CO)_3(\eta^1\text{-P-P})(\eta^2\text{-P-P})$ complexes exhibit one-electron-redox reactions characteristic of *fac* and *mer* tricarbonyl complexes studied previously.[7,9,11,12] Oxidation of the mer^+ species formed from each complex leads

---

(19) Colton, R. *Coord. Chem. Rev.* **1971**, *6*, 269.
(20) Colton, R.; Tomkins, I. B. *Aust. J. Chem.* **1966**, *19*, 1143.
(21) Colton, R.; Tomkins, I. B. *Aust. J. Chem.* **1966**, *19*, 1519.
(22) Anker, M. W.; Colton, R.; Tomkins, I. B. *Aust. J. Chem.* **1967**, *20*, 9.
(23) Bowden, J. A.; Colton, R. *Aust. J. Chem.* **1968**, *21*, 2657.
(24) Anker. M. W.; Colton, R.; Tomkins, I. B. *Aust. J. Chem.* **1968**, *21*, 1159.
(25) Anker, M. W.; Colton, R.; Tomkins, I. B. *Aust. J. Chem.* **1968**, *21*, 1143.
(26) Hanckel, J. M.; Darensbourg, M. Y. *J. Am. Chem. Soc.* **1983**, *105*, 6979.
(27) The periodic group notation in parentheses is in accord with recent actions by IUPAC and ACS nomenclature committees. A and B notation is eliminated because of wide confusion. Groups IA and IIA become groups 1 and 2. The d-transition elements comprise groups 3 through 12, and the p-block elements comprise groups 13 through 18. (Note that the former Roman number designation is preserved in the last digit of the new numbering: e.g., III → 3 and 13.)

to the formation of a divalent species that displays far less stability for chromium complexes than for those of molybdenum and tungsten.

There are two pathways which generate Mo(II) and W(II) dpe complexes—direct oxidation of *mer*-$[M(CO)_3(\eta^1\text{-dpe})(\eta^2\text{-dpe})]^+$ or the disproportionation of this complex. The *fac*- and *mer*-$M(CO)_3(\eta^1\text{-dpm})(\eta^2\text{-dpm})$ (M = Mo, W) complexes display rather different behavior with no evidence seen for a M(I) intermediate. However, the first oxidation for dpe and dpm complexes occurs at similar potentials (and very different from the second oxidation for the dpe compounds), which strongly suggests that the initial product of oxidation is $[M(CO)_3(\eta^1\text{-dpm})(\eta^2\text{-dpm})]^+$, which then very rapidly disproportionates to M(0) and M(II) by the process described in eq 5, which would result in an apparent two-electron-oxidation process on the coulometric time scale. It would be expected that formation of the seven-coordinate $[M(CO)_3(\eta^2\text{-P-P})_2]^{2+}$ from $[M(CO)_3(\eta^1\text{-P-P})(\eta^2\text{-P-P})]^+$ would be more efficient with dpm than with dpe because the pendant phosphorus would be close to the metal because of the geometry of the ligand. In the case of the much more flexible dpe ligand it is probable that significant molecular rearrangement would be necessary before the second dpe ligand chelates to the metal. Since the disproportionation of *mer*-$[M(CO)_3(\eta^1\text{-P-P})(\eta^2\text{-P-P})]^+$ simply involves electron transfer between similar molecules, which is known to be extremely fast for similar compounds,[11,12] it is likely that coordination of the free phosphorus is the rate-determining step in the overall disproportionation reaction and thus dpm complexes would be expected to disproportionate faster than the dpe complexes. Hence the apparent electrochemical differences between dpm and dpe complexes of molybdenum and tungsten are due to differences in the stability of M(I) complexes toward disproportionation.

The greater differences between chromium and the other two metals lies in the fact that seven-coordinate Cr(II) compounds are not readily formed, and this removes the driving force for the disproportionation reaction to proceed, thus giving rise to stable Cr(I) complexes. Although the seven-coordinate $[Cr(CO)_3(\eta^2\text{-dpm})_2]^{2+}$ cation is very unstable, being only observed at low temperature on the voltammetric time scale, it is presumably more stable than its 16-electron precursor $[Cr(CO)_3(\eta^1\text{-dpm})(\eta^2\text{-dpm})]^{2+}$. No evidence could be found for the corresponding seven-coordinate dpe cation. Presumably, the slower rate of chelation of the second ligand for dpe, discussed above, allows complete decomposition of $[Cr(CO)_3(\eta^1\text{-dpe})(\eta^2\text{-dpe})]^{2+}$, in a manner analogous to that shown in eq 2, before the second dpe ligand can chelate.

Acknowledgment. We thank Desma Page and Tony Hollenkamp for their valuable assistance in obtaining the electrochemical data.

Registry No. *fac*-$W(CO)_3(\eta^1\text{-dpm})(\eta^2\text{-dpm})$, 93401-93-5; *fac*-$Mo(CO)_3(\eta^1\text{-dpm})(\eta^2\text{-dpm})$, 56009-06-4; *fac*-$W(CO)_3(\eta^1\text{-dpe})(\eta^2\text{-dpe})$, 102132-79-6; *fac*-$Mo(CO)_3(\eta^1\text{-dpe})(\eta^2\text{-dpe})$, 97202-31-8; *fac*-$Cr(CO)_3(\eta^1\text{-dpe})(\eta^2\text{-dpe})$, 102132-78-5; *mer*-$W(CO)_3(\eta^1\text{-dpm})(\eta^2\text{-dpm})$, 93453-38-4; *mer*-$Mo(CO)_3(\eta^1\text{-dpm})(\eta^2\text{-dpm})$, 56085-32-6; *mer*-$Cr(CO)_3(\eta^1\text{-dpm})(\eta^2\text{-dpm})$, 93401-94-6; *mer*-$W(CO)_3(\eta^1\text{-dpe})(\eta^2\text{-dpe})$, 102209-57-4; *mer*-$Mo(CO)_3(\eta^1\text{-dpe})(\eta^2\text{-dpe})$, 102209-56-3; *mer*-$Cr(CO)_3(\eta^1\text{-dpe})(\eta^2\text{-dpe})$, 102209-55-2; *mer*-$[W(CO)_3(\eta^1\text{-dpe})(\eta^2\text{-dpe})]^+$, 102132-85-4; *mer*-$[Mo(CO)_3(\eta^1\text{-dpe})(\eta^2\text{-dpe})]^+$, 102132-83-2; *mer*-$[Cr(CO)_3(\eta^1\text{-dpe})(\eta^2\text{-dpe})]^+$, 102132-80-9; *mer*-$[Cr(CO)_3(\eta^1\text{-dpm})(\eta^2\text{-dpm})]^+$, 98152-90-0; $[W(CO)_3(\eta^2\text{-dpm})_2]^{2+}$, 102132-82-1; $[Mo(CO)_3(\eta^2\text{-dpm})_2]^{2+}$, 102132-81-0; $[Cr(CO)_3(\eta^2\text{-dpm})_2]^{2+}$, 102153-35-5; $[W(CO)_3(\eta^2\text{-dpe})_2]^{2+}$, 102132-86-5; $[Mo(CO)_3(\eta^2\text{-dpe})_2]^{2+}$, 102132-84-3; $(C_7H_8)W(CO)_3$, 12128-81-3; $(C_7H_8)Mo(CO)_3$, 12125-77-8; $(C_7H_8)Cr(CO)_3$, 12125-72-3.

Contribution from the Department of Chemistry,
University of Georgia, Athens, Georgia 30602

Dialkylamino Phosphorus Metal Carbonyls. 1. Mononuclear Derivatives from Reactions of Bis(diisopropylamino)phosphine with Metal Carbonyls[1]

R. B. King* and W.-K. Fu

Received October 11, 1985

Reactions of $(i\text{-}Pr_2N)_2PH$ with the tetrahydrofuran complexes $(THF)M(CO)_n$ (n = 4, M = Fe; n = 5, M = Cr, Mo, W) and $(THF)Mn(CO)_2Cp$ give the corresponding $(i\text{-}Pr_2N)_2PHM(CO)_n$ and $(i\text{-}Pr_2N)_2PHMn(CO)_2Cp$ complexes as air-stable sublimable hydrocarbon-soluble solids. A similar reaction of $(i\text{-}Pr_2N)_2PH$ with *fac*-$(EtCN)_3W(CO)_3$ results in ligand redistribution to give *cis*-$[(i\text{-}Pr_2N)_2PH]_2W(CO)_4$. In general these $(i\text{-}Pr_2N)_2PH$ complexes react rapidly with the hydrogen halides HX (X = Cl, Br) to cleave selectively in good yield one of the two diisopropylamino groups to give the corresponding $i\text{-}Pr_2NP(H)X$ complexes; the exception to this reactivity pattern is the reaction of $(i\text{-}Pr_2N)_2PHMn(CO)_2Cp$ with HBr, which proceeds all the way to $Br_2P(H)Mn(CO)_2Cp$. Methanolyses of $Br_2P(H)Mn(CO)_2Cp$ and $(i\text{-}Pr_2N)_2PHMn(CO)_2Cp$ give $(MeO)_2PHMn(CO)_2Cp$ and $i\text{-}Pr_2NP(H)(OMe)Mn(CO)_2Cp$, respectively; treatment of the latter complex with HCl gives $MeOP(H)ClMn(CO)_2Cp$. Dehydrochlorination of $i\text{-}Pr_2NP(H)ClFe(CO)_4$ with excess triethylamine gives a low yield of the phosphorus-bridging carbonyl derivative $(i\text{-}Pr_2NP)_2COFe_2(CO)_6$, previously obtained from the reaction of $Na_2Fe(CO)_4$ with $i\text{-}Pr_2NPCl_2$. The infrared ν(CO) spectra and the proton, phosphorus-31, and carbon-13 NMR spectra of the new complexes are described.

Introduction

Bis(diisopropylamino)phosphine, $(i\text{-}Pr_2N)_2PH$, has recently become readily available[2] through the $LiAlH_4$ reduction of $(i\text{-}Pr_2N)_2PCl$. Metal carbonyl complexes of $(i\text{-}Pr_2N)_2PH$ are of interest because they contain potentially reactive phosphorus–hydrogen and phosphorus–nitrogen bonds. This paper describes a number of mononuclear $(i\text{-}Pr_2N)_2PH$ metal carbonyl complexes as well as the cleavage of one or, in one case, both phosphorus–nitrogen bonds in such complexes with hydrogen halides to give the corresponding metal carbonyl complexes of the ligands $i\text{-}Pr_2NP(H)X$ (X = Cl, Br) and Br_2PH. Subsequent papers of this series discuss the formation of $(i\text{-}Pr_2N)_2P$ and $i\text{-}Pr_2NP$ metal carbonyl derivatives from $(i\text{-}Pr_2N)_2PH$ and the binuclear metal carbonyls $Mn_2(CO)_{10}$ and $Co_2(CO)_8$ as well as the nucleophilic substitution of the reactive halogen atoms in $i\text{-}Pr_2NP(H)X$ metal carbonyl complexes with the reactive transition-metal nucleophile $C_5H_5Fe(CO)_2^-$ to give novel heterobimetallic derivatives.

---

(1) (a) Portions of this work were presented at the 12th International Conference on Organometallic Chemistry, Vienna, Austria, Sept 1985, and the 190th National Meeting of the American Chemical Society, Chicago, IL, Sept 1985. (b) For a preliminary communication on this work see: King, R. B.; Fu, W.-K. *J. Organomet. Chem.* **1984**, *272*, C33.

(2) King, R. B.; Sundaram, P. M. *J. Org. Chem.* **1984**, *49*, 1784.

0020-1669/86/1325-2384\$01.50/0 © 1986 American Chemical Society